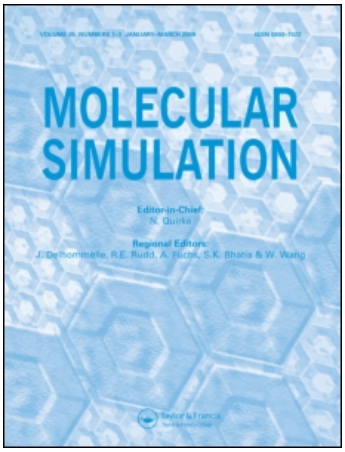

Molecular Simulation
Publication details, including instructions for authors and subscription information:
http://www.informaworld.com/smpp/title~content=t713644482

Simulations of the Thermal Conductivity in the Vicinity of the Critical Point

Debra J. Searles[ab]; Denis J. Evans[a]; Howard J. M. Hanley[c]; Sohail Murad[d]
[a] Research School of Chemistry, The Australian National University, Canberra, Australia [b] Department of Chemistry, The University of Queensland, Queensland, Australia [c] Physical and Chemical Properties Division, National Institute of Standards and Technology, Boulder, Colorado, USA [d] Department of Chemical Engineering, University of Illinois, Chicago, Illinois, USA

To cite this Article Searles, Debra J. , Evans, Denis J. , Hanley, Howard J. M. and Murad, Sohail(1998) 'Simulations of the Thermal Conductivity in the Vicinity of the Critical Point', Molecular Simulation, 20: 6, 385 — 395
To link to this Article: DOI: 10.1080/08927029808022045
URL: http://dx.doi.org/10.1080/08927029808022045

Molecular Simulation, 1998, Vol. 20, pp. 385–395
Reprints available directly from the publisher
Photocopying permitted by license only

SIMULATIONS OF THE THERMAL CONDUCTIVITY IN THE VICINITY OF THE CRITICAL POINT

DEBRA J. SEARLES[a,*], DENIS J. EVANS[a],
HOWARD J. M. HANLEY[b] and SOHAIL MURAD[c]

[a] *Research School of Chemistry, The Australian National University, Canberra, ACT 0200, Australia;*
[b] *Physical and Chemical Properties Division, National Institute of Standards and Technology, Boulder, Colorado, USA;*
[c] *Department of Chemical Engineering, University of Illinois, Chicago, Illinois, USA*

(Received in final form October 1997)

Isothermal-isobaric nonequilibrium molecular dynamics and Green-Kubo simulations are developed and used to calculate the thermal conductivity of an 864 particle Lennard-Jones fluid, with one simulation for 6912 particles, in the vicinity of the critical point. A small enhancement of the conductivity is observed. The isothermal compressibility is also evaluated. Agreement between the simulated data and the isothermal compressibility of argon is excellent.

Keywords: Nonequilibrium molecular dynamics simulation; thermal conductivity; isothermal compressibility; critical point phenomena

1. INTRODUCTION

In this paper we report preliminary simulation results for the behavior of the thermal conductivity coefficient, λ, of an 864 particle Lennard-Jones fluid in the vicinity of the critical point. The calculations are of interest because numerous authors have established experimentally that the thermal conductivity coefficient diverges as the critical point is approached. In fact, data obtained by heat transfer and/or light scattering techniques are

* Present address: Department of Chemistry, The University of Queensland, Brisbane, Queensland 4072, Australia.

available for such diverse fluids as argon, carbon dioxide, steam, hydrogen, methane, helium, ammonia and the refrigerant R134a [1, 2]. In general, if variables $\Delta\tilde{T}$ and $\Delta\tilde{\rho}$ are defined by

$$\begin{aligned} \Delta\tilde{T} &= (T - T_c)/T_c \\ \Delta\tilde{\rho} &= (\rho - \rho_c)/\rho_c \end{aligned} \tag{1}$$

where ρ is the mass density, T is the temperature and the subscript c denotes the critical value, it is found that the anomalous conductivity is observed in the approximate range $|\Delta\tilde{T}| \leq 1/3$ and $|\Delta\tilde{\rho}| \leq 2/3$. Figure 1 for the conductivity of carbon dioxide, extracted from Ref. [1], is a well known example.

At the outset we acknowledge that it has been shown that the location of the critical point of a Lennard-Jones system, or any other potential model, is

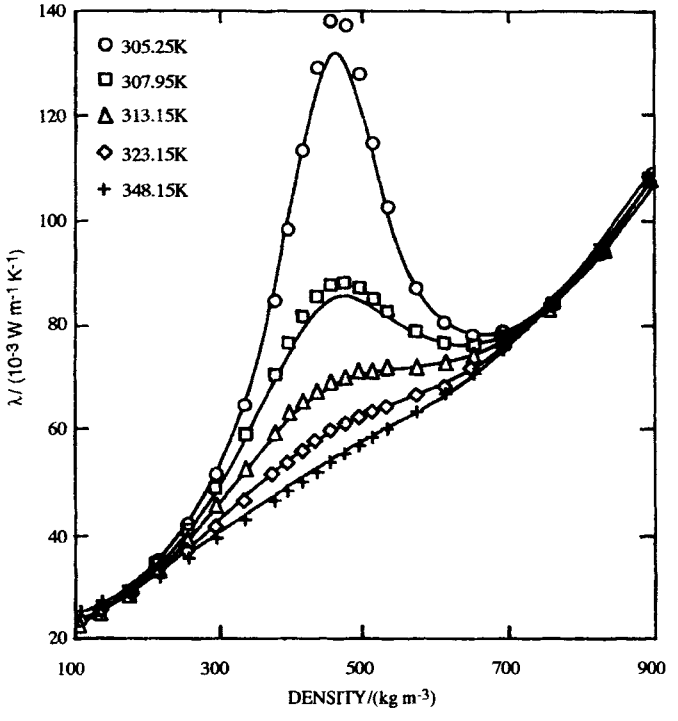

FIGURE 1 The thermal conductivity of carbon dioxide in the vicinity of the critical point ($\rho_c = 467.8$ kg/m^3, $T_c = 304.13$ K) extracted from the work of Sengers [1] and reproduced by permission.

especially sensitive to the number of particles, N, and the potential cut-off distance, r_{cut} [3, 4]. But we stress that an investigation of the variation of the Lennard-Jones critical point with N, and r_{cut}, and the possible variation of the thermal conductivity, is not an objective here; the calculations become very lengthy otherwise. Accordingly, we focused this study on a system with $N = 864$ and $r_{cut} = 3.379$, with respect to only one set of critical parameters, namely the critical temperature and density values from the equation of state of Nicholas *et al.* [5] (T_c and $\rho_c = 0.35$), recognizing that these values may not apply exactly to our systems. The constraint can be monitored, however, by evaluating, under the same conditions used to calculate the thermal conductivity, the isothermal compressibility, κ_T:

$$\kappa_T = \left(-\frac{\partial \ln V}{\partial p} \right)_T = -\frac{1}{k_B T V} \langle \Delta \widehat{V}^2 \rangle_p \tag{2}$$

where V is the average volume of the system at pressure p, and k_B Boltzmann's constant. The compressibility can be found relatively easily either by simple differentiation along an isotherm or by evaluating the fluctuations in volume, $\langle \Delta \widehat{V}^2 \rangle_p$. We argue that if the calculated κ_T displays an enhancement around our selected T_c and ρ_c, these critical parameters must be reasonable.

2. SIMULATION ALGORITHMS

Computer simulations of the thermal conductivity coefficient are relatively scarce, but methods to simulate transport properties in general have improved substantially over the last few years, largely because of the versatility and success of the technique of nonequilibrium molecular dynamics (NEMD) and because simulation algorithms are available that are no longer restricted to the microcanonical ensemble [6, 7]. In fact, the equations of motion and the algorithms used in this work are now standard [7–10].

The equilibrium and nonequilibrium molecular dynamic simulations were carried out in an isobaric-isothermal ensemble with a Nosé-Hoover constraint used to maintain the pressure and a Gaussian constraint to maintain the temperature [7, 8]. The isobaric-isothermal, rather that the more conventional isochoric-isothermal ensemble, was selected mainly because we wanted to evaluate the isothermal compressibility directly from Equation (2).

2.1. Equilibrium MD

All calculations, for MD and NEMD, were performed for a system of N particles of mass m in simulation volume V characterized by the two-body Lennard-Jones potential,

$$U(r) = 4\varepsilon\left(\left(\frac{\sigma}{r}\right)^{12} - \left(\frac{\sigma}{r}\right)^{6}\right), \quad r < r_{\text{cut}} \tag{3}$$
$$= 0, \quad r \geq r_{\text{cut}}$$

where $r = r_{ij} = |\boldsymbol{r}_i - \boldsymbol{r}_i|$ for all particles i and j; ε and σ are the energy and size potential parameters but, as is usual practice, we set $\varepsilon = 1$, $m = 1$ and $\sigma = 1$.

The equations of motion for the equilibrium isobaric-isothermal simulations are [7],

$$\begin{aligned} \dot{\boldsymbol{q}}_i &= \boldsymbol{p}_i/m + \dot{\varepsilon}\,\boldsymbol{q}_i \\ \dot{\boldsymbol{p}}_i &= \boldsymbol{F}_i - \dot{\varepsilon}\,\boldsymbol{p}_i - \alpha\,\boldsymbol{p}_i \\ \dot{V} &= 3\,\dot{\varepsilon}V \end{aligned} \tag{4}$$

where $\boldsymbol{q}_i$ and $\boldsymbol{p}_i$ are the coordinates and peculiar momenta for each particle, i, and the force is given by $\boldsymbol{F}_i = -\sum_{j \neq i} \nabla_{r_i} U(\boldsymbol{r}_{ij})$. The dilation rate $\dot{\varepsilon}$ is treated as a a Nosé-Hoover constraint parameter, where

$$\ddot{\varepsilon} = \frac{(\widehat{p} - p)\,V}{QNk_B\,T} \tag{5}$$

with $\widehat{p}$ the instantaneous pressure and p the target pressure. The term Q is a damping constant which determines the extent of the pressure fluctuations. It has been shown that time averaged properties are insensitive to the value of Q [8].

The quantity α in Eq. (4) is Gaussian multiplier given by the expression,

$$\alpha = -\dot{\varepsilon} + \frac{\sum_{i=1}^{N} \boldsymbol{F}_i \bullet \boldsymbol{p}_i}{\sum_{i=1}^{N} \boldsymbol{p}_i^2} \tag{6}$$

The thermal conductivity coefficient follows from the Green-Kubo expression modified for the isobaric-isothermal ensemble:

$$\lambda = \frac{1}{3Vk_B\,T^2}\int_0^{\infty} dt\,\langle \widehat{\boldsymbol{J}}_Q(t)\,\widehat{V}(t) \bullet \widehat{\boldsymbol{J}}_Q(0)\,\widehat{V}(0)\rangle_p \tag{7}$$

where $\widehat{V}(t)$ is the instantaneous volume at time t and the heat flux vector,

$\hat{\boldsymbol{J}}_Q$ is given by,

$$\hat{\boldsymbol{J}}_Q \hat{V} = \sum_{i=1}^{N} \frac{\boldsymbol{p}_i}{m} \hat{e}_i - \frac{1}{2} \sum_{i,j} \boldsymbol{q}_{ij} \boldsymbol{F}_{ij} \bullet \frac{\boldsymbol{p}_i}{m} \tag{8}$$

where $\hat{e}_i$ is the instantaneous energy of particle i: $\hat{e}_i = \frac{1}{2}\sum_i p_i^2 + \frac{1}{2}\sum_{i \neq j} U(r_{ij})$.

2.2. Nonequilibrium MD

Our NEMD algorithm is a straightforward adaptation of that developed by Evans in 1982 [9] modified for the isochoric-isothermal ensemble. The key to the algorithm is to impose on the system a fictitious heat field vector, $\boldsymbol{F}_Q$ which gives rise to the heat flux $\boldsymbol{J}_Q$. It can be shown that in the limit of zero field, the time average of the nonequilibrium steady state ratio of the flux to the field gives the thermal conductivity for the equilibrium system,

$$\lambda = \lim_{F_Q \to 0} \frac{\langle \hat{\boldsymbol{J}}_Q \hat{V} \rangle_p}{TV\boldsymbol{F}_Q^2} \bullet \boldsymbol{F}_Q \tag{9}$$

The equations of motion in the isobaric ensemble are

$$\begin{aligned} \dot{\boldsymbol{q}}_i &= \boldsymbol{p}_i/m + \dot{\varepsilon}\, \boldsymbol{q}_i \\ \dot{\boldsymbol{p}}_i &= \boldsymbol{F}_i + (\hat{e}_i - e)\, \boldsymbol{F}_Q - \frac{1}{2}\sum_j \boldsymbol{F}_{ij}(\boldsymbol{q}_{ij} \bullet \boldsymbol{F}_Q) + \frac{1}{2N}\sum_{j,k} \boldsymbol{F}_{jk}(\boldsymbol{q}_{ij} \bullet \boldsymbol{F}_Q) - \dot{\varepsilon}\, \boldsymbol{p}_i - \alpha \boldsymbol{p}_i \\ \dot{V} &= 3\dot{\varepsilon}\, V \end{aligned} \tag{10}$$

where e is the average energy per particle: $e = \frac{1}{N}\sum_{i=1}^{N} \hat{e}_i$. The Nosé-Hoover multiplier $\dot{\varepsilon}$ is given by Eq. (5) and the Gaussian multiplier now becomes

$$\alpha = -\dot{\varepsilon} + \frac{\sum_{i=1}^{N} \boldsymbol{p}_i \bullet \left(\boldsymbol{F}_i + (\hat{e}_i - e)\boldsymbol{F}_Q - \frac{1}{2}\sum_j \boldsymbol{F}_{ij}(\boldsymbol{q}_{ij} \bullet \boldsymbol{F}_Q) + \frac{1}{2N}\sum_{j,k} \boldsymbol{F}_{jk}(\boldsymbol{q}_{ij} \bullet \boldsymbol{F}_Q) \right)}{\sum_{i=1}^{N} \boldsymbol{p}_i^2} \tag{11}$$

3. RESULTS AND DISCUSSION

As stated, we assumed that the critical temperature and density were the values given by Nicholas *et al.* [5] and the simulations were carried out for the "critical isotherm" (at temperature $T_c = 1.35$) over a range of densities

spanning the Nicholas *et al.* critical density, $\rho_c = 0.35$. We also report data for the isotherm $T = 2.5$ ($\sim 1.9\ T_c$), so chosen to give a series of background thermal conductivities so that any critical enhancement of the conductivity could be highlighted, see below. The isothermal compressibility was also calculated at each state point, but it was found that it was best to estimate this property from the fluctuations in density or volume, Eq. (2).

All equilibrium and nonquilibrium MD simulations were carried out in a periodic cubic cell with a timesteps of 0.001 or 0.002. Target temperatures and densities were selected and the pressure for each state point was determined using an isochoric-isothermal simulation. The pressure was then constrained at the calculated value and the simulation continued under isobaric-isothermal conditions. To constrain the pressure, a value of $Q/NkT = 100$ was selected by trial and error although, as remarked, the choice of Q was, apart from questions of computational efficiency, unimportant. For the equilibrium simulations, the thermal conductivity was determined using the Green-Kubo integral of the dissipative flux (Eq. 7). Simulations at each state point were run for at least 10^3 reduced time units, during which time correlation functions were calculated in the time domain, $0 < t < 10$. For the NEMD simulations, a field was applied in the x-direction: $\boldsymbol{F}_Q = \boldsymbol{i}F_{Qx}$. For each state point, a minimum of four different field strengths between 0.01 and 0.15 were used and the conductivity estimated from Eq. (9) after extrapolation to zero field by fitting an even quadratic polynomial to the field-dependent data. Simulation times for the NEMD simulations ranged from $t = 200$ to $t = 6000$ for each field, with longer simulations required for the low field calculations.

Figure 2 displays the calculated isothermal compressibility and it is seen that there is a sharp increase around the selected critical density at the selected critical temperature, substantiating that our choice of T_c and ρ_c is not unreasonable. As a matter of interest, κ_T for argon was estimated at corresponding reduced temperatures and densities from the equation of state of McCarty *et al.* [11] and reduced by the Lennard-Jones parameters $\sigma = 0.341$ nm and $\varepsilon/k_B = 119.8$ K [12]. Considering the imprecision in our choice of critical parameters, agreement is excellent.

The critical isotherm simulations are presented in terms of a critical excess conductivity, $\Delta\lambda_c(\rho, T)$, defined as follows. If contributions to the thermal conductivity from the influence of the critical point can be neglected, one can write a density and temperature dependent excess conductivity $\Delta\lambda_b(\rho, T)$:

$$\Delta\lambda_b(\rho, T) = \lambda_b(\rho, T) - \lambda_0(T)$$

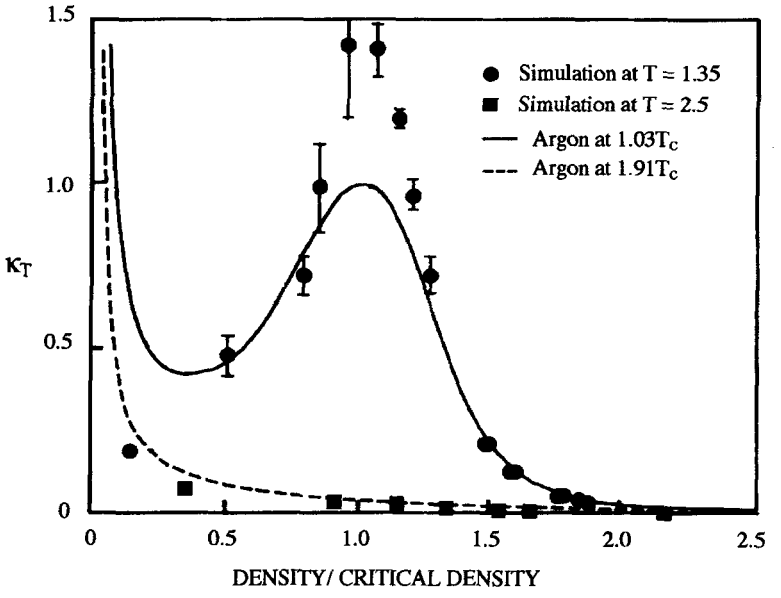

FIGURE 2 Simulated values of the isothermal compressibility at $T=2.5$ (filled sqares) and $T=1.35$ (filled circles) estimated from the fluctuations in volume, Equation (2). The curves are argon data from the equation of state of McCarty [11] reduced by the Lennard Jones potential parameters [12].

or, trivially

$$\lambda_b(\rho, T) = \lambda_0(T) + \Delta\lambda_b(\rho, T), \qquad |(\Delta\tilde{\rho}, \Delta\tilde{T})| \gg 0 \tag{12}$$

where, $\lambda_0(T)$, is the dilute gas, density independent, thermal conductivity and $\lambda_b(\rho, T)$ is the total conductivity with $|(\Delta\tilde{\rho}, \Delta\tilde{T})| \gg 0$. Close to the critical point, however,$|(\Delta\tilde{\rho}, \Delta\tilde{T})| \to 0$ but Eq. (12) can be extended to become,

$$\lambda(\rho, T) = \lambda_0(T) + \Delta\lambda_b(\rho, T) + \Delta\lambda_c(\rho, T) \qquad |(\Delta\tilde{\rho}, \Delta\tilde{T})| \to 0 \tag{13}$$

hence defining the excess $\Delta\lambda_c(\rho,T)$.

Equation (13) is convenient because experiment indicates that the excess background conductivity depends strongly on the density but only weakly on the temperature [13]. Thus, to a first approximation, $\Delta\lambda_b(\rho,T) \approx \Delta\lambda_b(\rho)$, provided $|(\Delta\tilde{\rho}, \Delta\tilde{T})| \gg 0$. Given, therefore, conductivity data in the vicinity of the critical point as a function of density at a particular temperature, we can estimate $\Delta\lambda_c(\rho, T)$ – and hence identify a possible critical enhancement

more clearly – since $\lambda_0\ (T)$ can be measured or calculated at the temperature and $\Delta\lambda_b\ (\rho,T)$ can be estimated from data outside the critical region.

Here the background thermal conductivity coefficients are the values at $T=2.5$ shown as Figure 3. The curve is a monotonic, fairly strong, function of density that extrapolates smoothly to the dilute gas value, $\lambda_0(T)$, calculated from the standard kinetic theory expression [12]. The equilibrium Green-Kubo (Eq. (7)) and the NEMD (Eq. (9)) data points are consistent well within their respective error bars. Again, as a matter of interest, we compare the simulated data with experiment. The 298.15 K set of data reported by Tiesinga *et al.* [2] were reduced with the Lennard Jones potential parameters [12] and plotted in Figure 3; agreement between the argon data and the simulation is very satisfactory.

The results for the $T=1.35$ isotherm are presented as a critical excess, $\Delta\lambda_c\ (\rho T)$. The background conductivity, $\Delta\lambda_b\ (\rho T)$, was estimated by fitting the $T=2.5$ data constrained to the dilute gas value. The background was

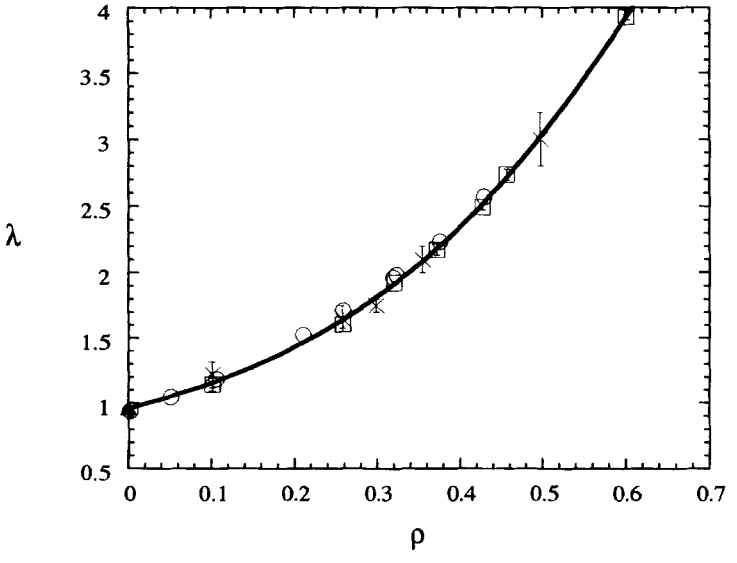

FIGURE 3 The thermal conductivity of a Lennard-Jones fluid as a function of density along the isotherm $T=2.5$, well above the critical point. The crosses are obtained from equilibrium MD simulations and the squares from NEMD. The curve is a fit through the simulated data constrained at the zero density, dilute gas, value which is shown as a filled triangle. The circles are argon data at 298.15 K from Ref. [2] reduced by Lennard-Jones parameters.

then subtracted from the $T = 1.35$ results to give the excess plotted in Figure 4. A weak enhancement – consistent in principle with experiment – is apparent. For the 864 particle system, we estimate that the error bars are $\pm$ 0.15 due to the uncertainty in the simulation and, to a lesser extent, the uncertainty in the subtraction. Thus, although we believe the enhancement to be real, the evidence is not clear-cut. We note, however, that the Green Kubo and the NEMD simulations give compatible results and we are satisfied that the simulation algorithms are correct. This small system size is of course a constraint, especially because the qualitative behavior of a fluid around the gas/liquid critical point can be explained successfully, notably by Sengers and coworkers [1, 6], in terms of the long-ranged fluctuations in the density that are characteristic of critical behavior. Clearly the fluctuations will be influenced by the choice of N.

To give an indication of the system size dependence of the critical enhancement, we carried out one simulation for a 6912 particle system at a density of $\rho = 0.32$. Although a slight increase in the critical enhancement

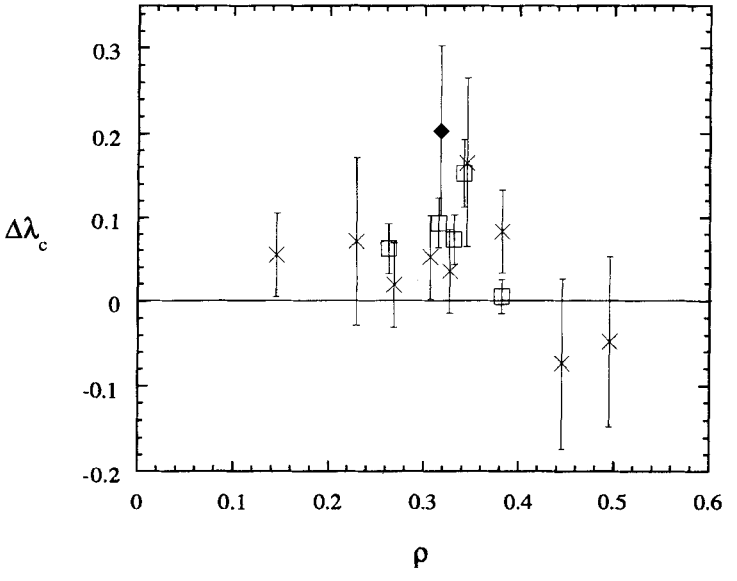

FIGURE 4 The critical excess thermal conductivity at $T = 1.35$ for the 864 particle system. See Equation (13). The background thermal conductivity was obtained from the fit of the density dependence of the thermal conductivity away from the critical point (see Fig. 3) and the Lennard-Jones dilute gas thermal conductivity was obtained from Ref. [11]. The filled diamond is the value for the 6912 particle system.

of the thermal conductivity is observed, a small additional enhancement is apparent.

In conclusion, we have generalised the usual isochoric equilibrium and nonequilibrium molecular dynamics algorithms for calculating the thermal conductivity. Calculations using these two algorithms are consistent and have verified that the computer simulations can predict an enhancement in the vicinity of the critical point. However, to relate the results more closely to experiment, we will require study of much larger systems, and the accurate location of the critical point as a function of system size. This is a formidable computational task.

Acknowledgements

The Department of Energy (Division of Chemical Sciences) provided support to Murad and Hanley for this work. Searles thanks the Australian Research Council for the award of an ARC Fellowship, Evans thanks the staff of the NIST Physical and Chemical Properties Division for their hospitality.

References

[1] A survey of thermal conductivity data and a discussion on their interpretation is given, for example, in: J. V. Sengers and J. Luettmer-Strathmann, "The Critical Enhancements" in *Transport properties of Fluids: Their Correlation, Prediction and Estimation* (J. Millat, J. H. Dymond, and C. A. Nieto de Castro, Eds.) Cambridge U. Press, 1996. Chap. 6.

[2] Tiesinga, B. W., Sakonidou, E. P., van den Berg, H. R., Luettmer-Strathmann, J. and Sengers, J. V. (1994). "The thermal conductivity of argon in the critical region", *J. Chem. Phys.*, **101**, 6944.

[3] Smit, B. (1992). "Phase diagrams of Lennard-Jones fluids", *J. Chem. Phys.*, **96**, 8639.

[4] Panagiotopoulos, A. Z. (1994). "Molecular simulation of phase coexistence: Finite-size effects and determination of critical parameters for two- and three-dimensional Lennard-Jones fluids", *Int. J. Thermophys.*, **15**, 1057.

[5] Nicolas, J. J., Gubbins, K. E., Street, W. B. and Tildesley, D. J. (1979). "Equation of state for the Lennard-Jones fluid", *Mol. Phys.*, **37**, 1429.

[6] Evans, D. J. and Morriss, G. P. (1984). "Non-Newtonian molecular dynamics", *Comp. Phys. Rep.*, **1**, 297.

[7] Evans, D. J. and Morriss, G. P. (1990). *Statistical Mechanics of Nonequilibrium Liquids*, Academic Press, London.

[8] Hood, L. M., Evans, D. J. and Hanley, H. J. M. (1989). "Properties of a soft-sphere liquid from non-Newtonian molecular dynamics", *J. Stat. Phys.*, **57**, 729; L. M. Hood, D. J. Evans and G. P. Morriss (1987). "Time correlation function in the stress ensemble", *Mol. Phys.*, **62**, 419.

[9] Evans, D. J. (1982). "Homogeneous NEMD algorithm for thermal conductivity – application of non-canonical linear response theory", *Phys. Lett.*, **91A**, 457.

[10] Hanley, H. J. M. and Evans, D. J. (1996). Chapter 9 "Transport properties and Nonequilibrium Molecular dynamics" in Transport properties of Fluids: Their *Correlation*,

Prediction and Estimation (J. Millat, J. H. Dymond and C. A. Nieto de Castro, Eds.) Cambridge U. Press, pp. 210–225.

[11] Younglove, B. A. (1982). "Thermophysical properties of fluids: argon, ethylene, parahydrogen, methane, nitrogen, nitrogen trifluoride and oxygen", *J. Phys. Chem. Ref. Data*, **11**, Supplement 1.

[12] Hirschfelder, J. O., Curtiss, C. F. and Bird, R. B. (1954). *Molecular Theory of Gases and Liquids*, Wiley & Sons, New York.

[13] Diller, D. E., Hanley, H. J. M. and Roder, H. M. (1970). "Density and temperature dependence of the viscosity and thermal conductivity of dense simple fluids", *Cryogenics*, **10**, 286.